

The 3a protein of severe acute respiratory syndrome-associated coronavirus induces apoptosis in Vero E6 cells

Patrick T. W. Law,^{1,2} Chi-Hang Wong,¹ Thomas C. C. Au,¹ Chi-Pang Chuck,² Siu-Kai Kong,² Paul K. S. Chan,³ Ka-Fai To,⁴ Anthony W. I. Lo,⁴ Judy Y. W. Chan,² Yick-Keung Suen,² H. Y. Edwin Chan,² Kwok-Pui Fung,^{2,5} Mary M. Y. Waye,^{2,5} Joseph J. Y. Sung,^{1,6} Y. M. Dennis Lo^{1,7} and Stephen K. W. Tsui^{1,2,5}

Correspondence
Stephen K. W. Tsui
kwtsui@cuhk.edu.hk

Centre for Emerging Infectious Diseases¹, Department of Biochemistry², Department of Microbiology³, Department of Anatomical and Cellular Pathology⁴, The Croucher Laboratory for Human Genomics⁵, Department of Medicine and Therapeutics⁶ and Department of Chemical Pathology⁷, The Chinese University of Hong Kong, Shatin, NT, Hong Kong SAR, China

Received 8 December 2004
Accepted 2 April 2005

An outbreak of severe acute respiratory syndrome (SARS) occurred in China and the first case emerged in mid-November 2002. The aetiological agent of this disease was found to be a previously unknown coronavirus, SARS-associated coronavirus (SARS-CoV). The detailed pathology of SARS-CoV infection and the host response to the viral infection are still not known. The 3a gene encodes a non-structural viral protein, which is predicted to be a transmembrane protein. In this study, it was shown that the 3a protein was expressed in the lungs and intestinal tissues of SARS patients and that the protein localized to the endoplasmic reticulum in 3a-transfected monkey kidney Vero E6 cells. *In vitro* experiments of chromatin condensation and DNA fragmentation suggested that the 3a protein may trigger apoptosis. These data showed that overexpression of a single SARS-CoV protein can induce apoptosis *in vitro*.

INTRODUCTION

Severe acute respiratory syndrome (SARS) has affected more than 8000 individuals and caused 774 deaths in 26 countries since the first case emerged in China in mid-November 2002 (<http://www.who.int/csr/sars/en/>). The aetiological agent of this disease was found to be a previously unknown coronavirus (SARS-associated coronavirus or SARS-CoV). The genomes of different strains of SARS-CoV have been sequenced (Marra *et al.*, 2003; Rota *et al.*, 2003; Ruan *et al.*, 2003; Tsui *et al.*, 2003; Yeh *et al.*, 2004) and found to contain 15 open reading frames (ORFs) encoding the replicase, four major structural proteins and several proteins of unknown function (Marra *et al.*, 2003).

The 3a locus (also known as X1 or ORF3; nt 25268–26092 in the Tor2 strain of SARS-CoV) encodes one of the ORFs of unknown function and is located between two structural genes encoding the spike and the envelope proteins of SARS-CoV (Marra *et al.*, 2003). Interestingly, the 3a ORF is not found in two human coronaviruses (OC43 and 229E) or other coronavirus species identified to date. This suggests that the 3a protein is a newly emerged protein in coronaviruses. In SARS-CoV-infected monkey kidney Vero E6 cells, 3a mRNA (Zeng *et al.*, 2003) and 3a protein (Yu *et al.*, 2004) have been detected. In addition, the 3a

protein has been detected in the lung tissue of a SARS patient (Yu *et al.*, 2004).

When the 3a sequence was searched against the SMART server (Letunic *et al.*, 2004), a predicted signal sequence was found at aa 1–16. In addition, three transmembrane domains were predicted at aa 34–56, 77–99 and 103–125. Furthermore, the C-terminal region of the 3a protein shares 53% (aa 209–264) and 40% (aa 152–254) similarity, respectively, with the *Plasmodium* calcium pump and the *Shewanella* outer-membrane porin. Notably, the outer-membrane porins are a family of bacterial proteins that may oligomerize to form transmembrane channels for the passive diffusion of small molecules across membranes.

Previous studies have shown that many coronaviruses, including murine hepatitis virus, avian infectious bronchitis virus and transmissible gastroenteritis coronavirus, are able to induce apoptosis of host cells (An *et al.*, 1999; Eléouët *et al.*, 2000; Liu *et al.*, 2001, 2003; Chen & Makino, 2002), but little is known about this ability in SARS-CoV. Apoptosis was observed in liver specimens from patients with SARS-associated viral hepatitis (Chau *et al.*, 2004) and lymphopenia is commonly observed in SARS patients and has been postulated to be caused by apoptosis induced by SARS-CoV infection (O'Donnell *et al.*, 2003). Although lymphopenia

may be a result of glucocorticoid treatment (Panesar *et al.*, 2004), it may also be due to the upregulation of apoptotic genes in SARS-CoV-infected human peripheral blood mononuclear cells, as shown by oligonucleotide array analysis (Ng *et al.*, 2004). Furthermore, SARS-CoV can induce a cytopathic effect and apoptosis (Yan *et al.*, 2004) in some cell-culture models, such as Vero E6 cells, and the nucleocapsid protein is able to induce apoptosis in COS-1 monkey kidney cells in the absence of growth factors (Surjit *et al.*, 2004). Recently, the ORF7a protein has been shown to induce apoptosis when overexpressed in Vero E6 cells (Tan *et al.*, 2004b). In the present study, we demonstrated that overexpression of the non-structural 3a protein triggers apoptosis in Vero E6 cells.

METHODS

Cell culture. Vero E6 cells were propagated in Dulbecco's modified Eagle's medium (Invitrogen Life Technologies) supplemented with 10% fetal bovine serum, penicillin G50 (100 U ml⁻¹) and streptomycin (100 µg ml⁻¹) at 37 °C in a 5% CO₂ incubator.

Immunohistochemistry. Sections of 4 µm were prepared from 10% formalin-fixed, routinely processed paraffin blocks of autopsy specimens. A standard avidin-biotin method was used for immunohistochemical studies, using antibodies specific for peptides of the nucleocapsid (N terminus, aa 1–17) and 3a (C terminus, aa 250–274) proteins (diluted 1:100) and pre-immune serum. Antibodies were generated from rabbits immunized with a keyhole limpet haemocyanin-conjugated synthetic peptide. Antigen retrieval was performed by microwave pre-treatment in 10 mM citrate buffer, pH 6.0, with preliminary heating at 780 W for 4 min, followed by 480 W twice for 5 min each.

Plasmid construction. To clone the 3a gene into pcDNA4/HisMaxTOPO (Invitrogen Life Technologies), the 3a ORF was amplified by using primers 3a-pcDNAF (5'-ATGGATTGTTTATGAGATTTTACTCTGG-3') and 3a-pcDNAR (5'-TTACAAA-GGCACGCTAGTAGTCGTCG-3'). cDNA prepared from the Su-10 coronavirus (Tsui *et al.*, 2003) was used as template. The PCR product was then ligated to linearized pcDNA4/HisMaxTOPO vector according to the manufacturer's protocol (Invitrogen Life Technologies) to produce the recombinant construct pcDNA4-3a. To prepare the recombinant construct pEGFP-3a, the 3a ORF was PCR-amplified by using the primers 3aC1F (5'-GCAGATCTATGG-ATTTGTTTATGAGATTTTACTCTTGGATC-3') and 3aC1R (5'-GCGGTACCTTACAAAGGCACGCTAGTAGTCGTCGTC-3'). The PCR product was digested with restriction enzymes (*Bgl*II and *Kpn*I) and ligated to the pEGFP-C1 vector [encoding a variant of wild-type green fluorescent protein (GFP); BD Biosciences Clontech].

Subcellular localization of the 3a protein. Vero E6 cells seeded on coverslips were co-transfected with 1 µg pcDNA4-3a and pDsRed2-ER (BD Biosciences Clontech) constructs. At 1 day post-transfection, cells were washed and fixed in 100% chilled methanol for 3 min. After blocking with 2% BSA in PBS for 30 min, cells were incubated with anti-3a antibody diluted 1:100 for 30 min. Cells were then washed three times with PBS. For fluorescent visualization, cells were incubated with fluorescein isothiocyanate (FITC)-conjugated anti-rabbit secondary antibody diluted in 1:500 in 2% BSA in PBS for 30 min. After washing five times with PBS, cell nuclei were stained with Hoechst 33342 (2.5 µg ml⁻¹ in PBS; Molecular Probes) for 30 min. Fluorescent signals were detected by using a Nikon TE2000U microscope and images were captured with the SPOT RT_{KE} imaging system (Diagnostic Instruments).

Overexpression of the 3a protein and Western blotting analysis. Approximately 1.7 × 10⁵ Vero E6 cells were transfected with 1 µg pcDNA4-3a or control plasmids in a six-well plate by using Lipofectamine PLUS reagent (Invitrogen Life Technologies). Cells were collected daily for 5 days, washed with 1 × PBS and trypsinized. The cell pellet was then resuspended in 100 µl lysis buffer [2% SDS, 10% glycerol, 0.0625 M Tris/HCl (pH 8.0)] and incubated on ice for 30 min. After boiling for 10 min and centrifugation at 12 000 g for 20 min, the supernatant was saved for protein quantification, polyacrylamide-gel electrophoresis and transfer to PVDF membrane (Millipore). The blot was incubated with primary antibody (diluted 1:1000) overnight and horseradish peroxidase-conjugated secondary antibody (diluted 1:1000) for 1 h. Antibodies used in this study for the detection of apoptotic markers were purchased from Santa Cruz Biotechnology, Sigma or Invitrogen Life Technologies. Signals were detected by using an Enhanced Chemiluminescence Western Blotting kit (Amersham Biosciences).

DNA-ladder analysis. Approximately 1.7 × 10⁵ Vero E6 cells were transfected with 1 µg pcDNA4-3a or control plasmids in a six-well plate by using Lipofectamine PLUS reagent (Invitrogen Life Technologies). Cells were collected daily for 5 days, washed with 1 × PBS and lysed in 400 µl lysis buffer [200 mM Tris (pH 8.3), 100 mM EDTA and 1% SDS] supplemented with 10 µl proteinase K (20 mg ml⁻¹). After incubation at 37 °C for 2 h, 150 µl saturated NaCl was added to the lysate and the mixture was shaken vigorously for 1 min. After centrifugation at 6500 g for 15 min, the supernatant was mixed with 1 ml ice-cold absolute ethanol and the mixture was subjected to centrifugation at 15 000 g for 20 min. The pellet was then washed with 1 ml ice-cold 75% ethanol and centrifuged at 7000 g for 5 min. The supernatant was discarded and the DNA pellet was allowed to dry in air. Finally, the pellet was resuspended in 20 µl RNase A solution (0.2 mg ml⁻¹) and incubated at 37 °C for 90 min. DNA fragmentation was then analysed in a 2% agarose gel.

Chromatin-condensation analysis and immunostaining. The recombinant constructs pEGFP-3a, pEGFP-C1 and pcDNA4-3a and the pcDNA4 empty vector were transfected independently into Vero E6 cells by using Lipofectamine PLUS reagent according to the manufacturer's protocol (Invitrogen Life Technologies). For chromatin-condensation analysis, cells were fixed in 4% paraformaldehyde and counterstained with either propidium iodide (1 mg ml⁻¹; Sigma) or Hoechst 33342 (2.5 µg ml⁻¹; Molecular Probes) in PBS for 30 min. For immunostaining, cells were treated as described above.

Terminal deoxynucleotidyl transferase-mediated dUTP nick end-labelling (TUNEL) assay. Approximately 1.7 × 10⁵ Vero E6 cells seeded on coverslips were transfected with pcDNA4-3a or pcDNA4 empty vector by using Lipofectamine PLUS reagent according to the manufacturer's protocol (Invitrogen Life Technologies). Cells were analysed for DNA fragmentation at 3–5 days post-transfection. Cells treated with DNase I (3000 U ml⁻¹) served as the positive control. Cells were fixed in 4% paraformaldehyde for 1 h and then treated with permeabilization solution (0.1% Triton X-100, 0.1% sodium citrate in PBS) for 5 min on ice. Cells were then incubated with a mixture of 45 µl labelling solution and 2 µl TUNEL reaction mix (Roche) in a humidified CO₂ incubator at 37 °C for 1 h. Cell nuclei were counterstained with 300 nM 4,6-diamidino-2-phenylindole (DAPI; Molecular Probes). Fluorescent signals were detected by using a Nikon TE2000U microscope and images were captured with the SPOT RT_{KE} imaging system (Diagnostic Instruments).

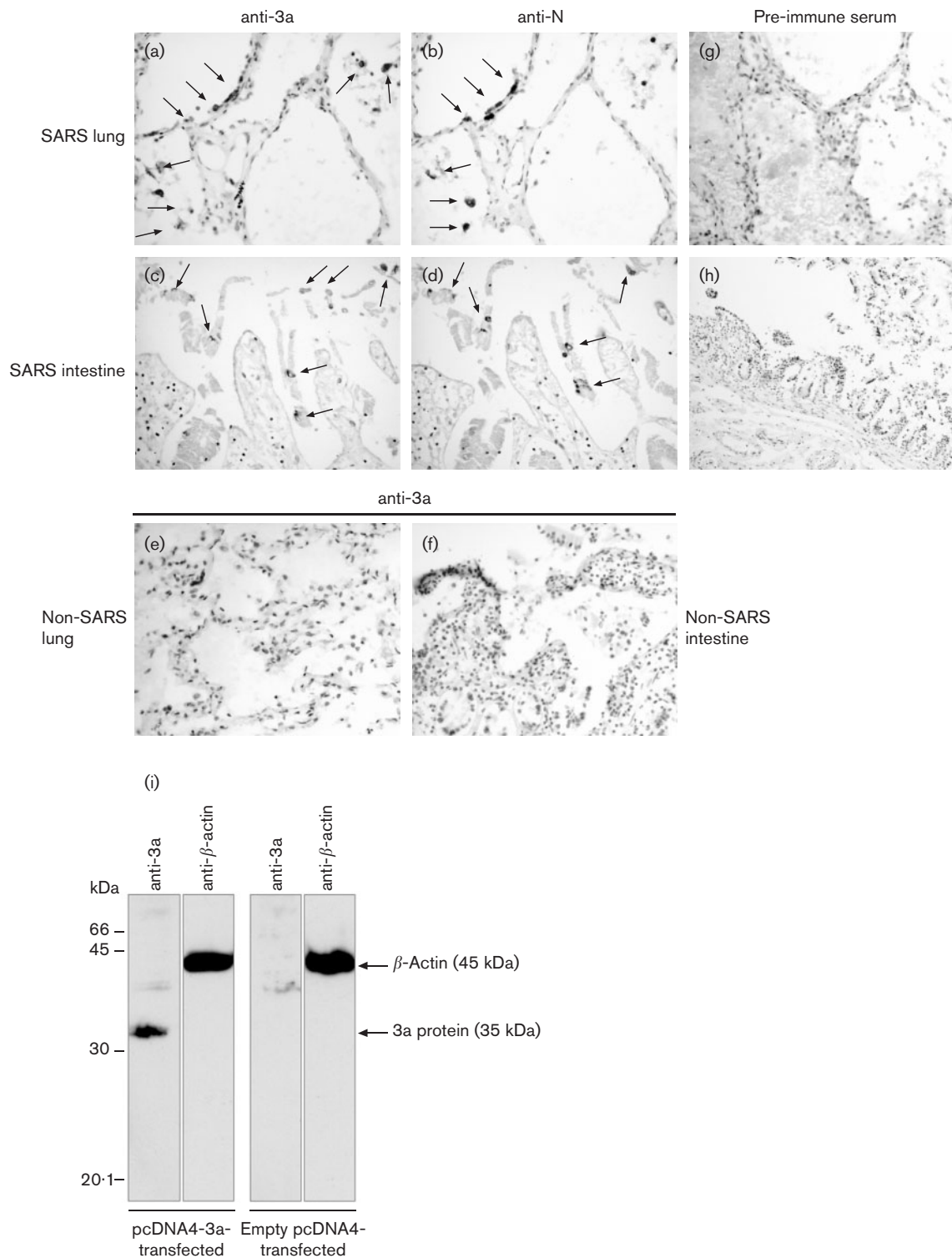


Fig. 1. Expression of SARS-CoV 3a protein. The 3a protein was detected in lung and intestinal tissues of fatal cases of SARS. Expression of the 3a protein was detected by immunohistochemical staining in SARS-CoV-infected pneumocytes (a, arrows) and surface enterocytes (c, arrows) in autopsy sections of SARS patients, showing strong cytoplasmic signals. Similar patterns of tissue distribution of the 3a and nucleocapsid proteins in SARS-CoV-infected cells (arrows) were demonstrated in serial sections of the lung (b) and intestine (d). The surface epithelium, especially in the small intestine, appeared to have detached due to autolysis. The specificity of anti-3a antibody was demonstrated in non-SARS pneumocytes (e) and non-SARS enterocytes (f). Immunostaining of infected pneumocytes and surface enterocytes, respectively, by using pre-immune serum is indicated in (g) and (h). In Western blot analysis, the anti-3a antibody was shown specifically to recognize a protein of the expected size (35 kDa) in the protein lysate of 3a-transfected Vero E6 cells (i).

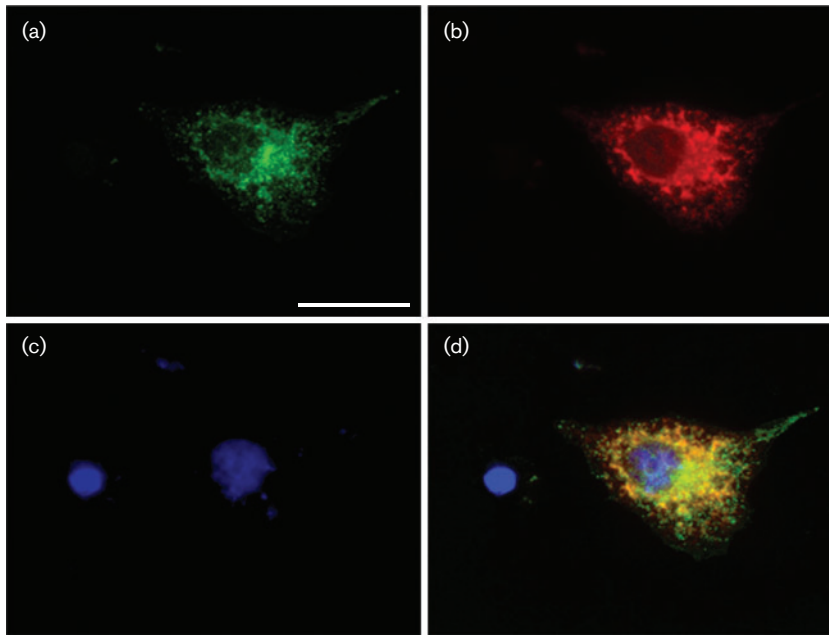


Fig. 2. Subcellular localization of the 3a protein in pcDNA4-3a-transfected Vero E6 cells. The 3a protein was co-expressed with DsRed2-ER and cells were immunostained with anti-3a antibody and visualized with an FITC-conjugated secondary antibody. (a) FITC fluorescent detection of the 3a protein, indicating the subcellular location of the ER. (b) Localization of DsRed2-ER tracker protein. (c) Hoechst 33342 staining showing the localization of the nucleus. (d) Overlay of fluorescent signals. Overlapping regions are displayed in yellow. Bar, 25 μ m.

RESULTS

Immunohistochemistry of the 3a protein

To examine expression of the 3a protein in SARS patients, we immunostained tissue sections with an anti-3a-specific peptide-raised antibody. Consistent with a previous

report (Yu *et al.*, 2004) and previous results on the tissue tropism of SARS-CoV (To *et al.*, 2004), we found 3a protein immunoreactivity in lung pneumocytes (Fig. 1a) and surface enterocytes in the terminal ileum of SARS patients (Fig. 1c). The signal pattern was similar to that of the nucleocapsid protein (Fig. 1b and d) and these

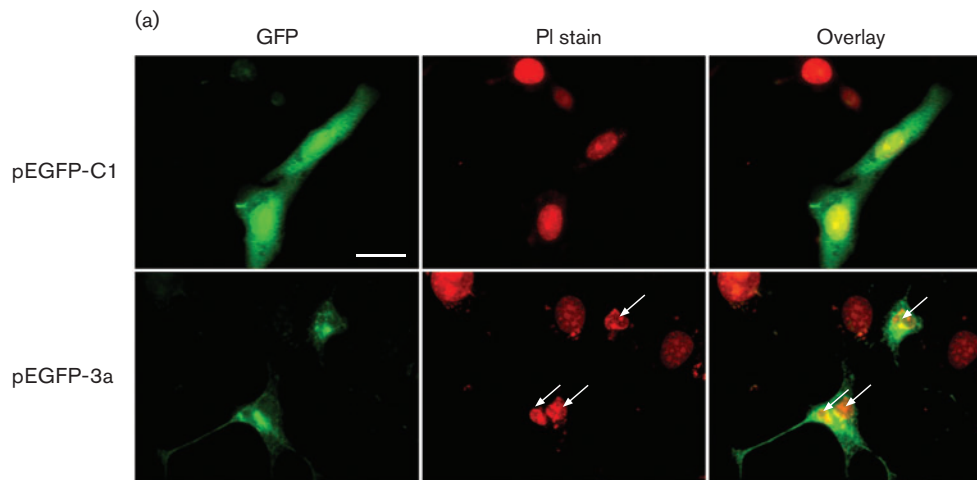
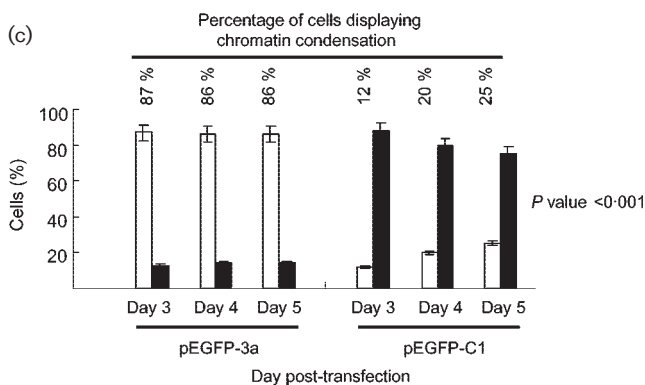
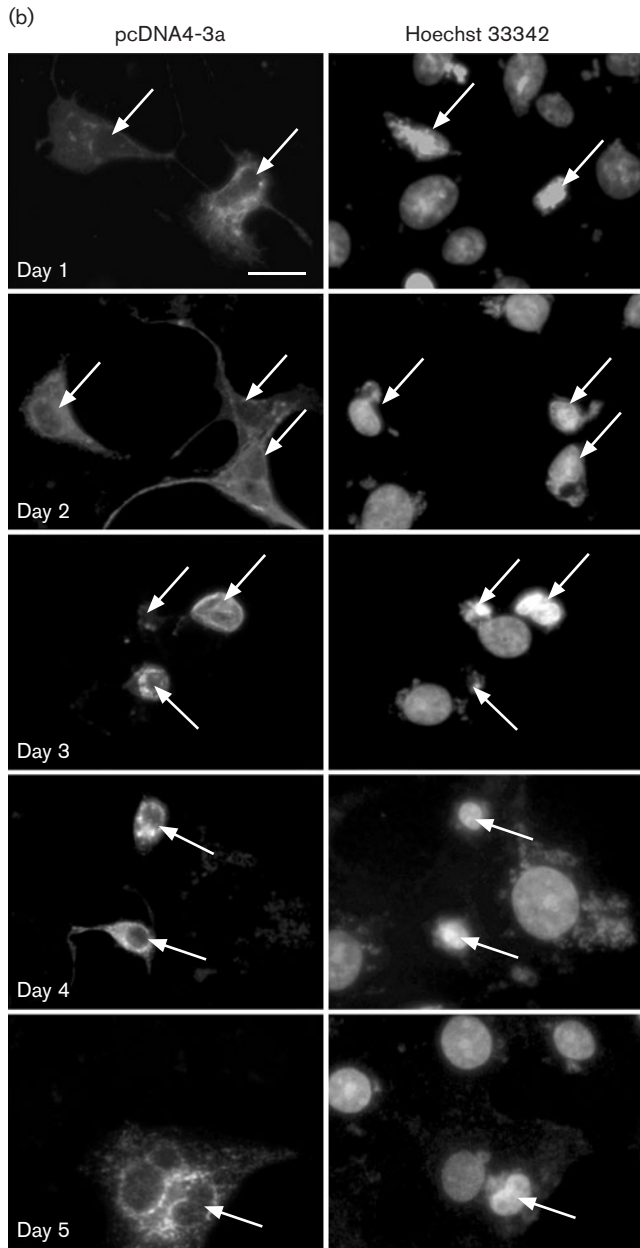


Fig. 3. Chromatin condensation in Vero E6 cells induced by the 3a protein. (a) Cells were transfected with pEGFP-C1 empty vector (upper panel) and pEGFP-3a (lower panel). GFP-positive cells with chromatin condensation are indicated by arrows. The overlay of the GFP and propidium iodide (PI) fluorescent signals is shown. (b) Immunostaining of pcDNA4-3a-transfected Vero E6 cells with anti-3a antibody from 1 to 5 days post-transfection. Cells were counterstained with Hoechst 33342 and immunoreactive cells with chromatin condensation are indicated by arrows. Bars, 25 μ m. (c) Effect of GFP-3a fusion protein on the induction of chromatin condensation in Vero E6 cells. Cells transfected with pEGFP-3a or pEGFP-C1 empty vector were monitored for nucleus condensation from 3 to 5 days post-transfection. Approximately 600 green fluorescent cells were counted and the proportion of cells with apoptotic nuclei was scored. The data shown are the means of three independent transfections. Empty bars, green fluorescent cells with chromatin condensation; filled bars, green fluorescent cells without chromatin condensation.



two cell types have consistently been found to harbour SARS-CoV. No immunoreactivity of the anti-3a antibody and pre-immune serum was detected in non-SARS (Fig. 1e

and f) or SARS (Fig. 1g and h) autopsies, respectively. By using Western blot analysis, we demonstrated that the anti-3a antibody specifically recognized a protein of 35 kDa corresponding to the expected size of the 3a protein (Fig. 1i).

Transient expression and subcellular localization of the 3a protein

To determine the subcellular localization of the 3a protein, pcDNA4-3a was co-expressed with the endoplasmic reticulum (ER)-specific construct DsRed2-ER in Vero E6 cells. At 1 day post-transfection, we observed a punctate fluorescent-signal pattern, similar to that of the ER, and co-localization of fluorescent signals from the ER-specific protein was observed (Fig. 2a–d).

Induction of chromatin condensation by the GFP-3a fusion construct

To investigate whether the 3a protein could induce apoptosis, Vero E6 cells were transfected with pEGFP-3a and morphological changes were examined by using an inverted fluorescent microscope. On day 3 post-transfection, extensive chromatin condensation, a hallmark of apoptosis, was observed in GFP-positive cells. These results indicated that the 3a protein induced apoptosis in Vero E6 cells (Fig. 3a). Similar results were observed when pcDNA4-3a-transfected Vero E6 cells were immunostained with anti-3a antibodies and counterstained with Hoechst 33342 (Fig. 3b). The overall transfection efficiency was approximately 28%. To correlate 3a protein expression with chromatin condensation in a more quantitative way and to confirm that shrinkage of the nucleus was not caused by GFP, the proportion of green-fluorescent cells with chromatin condensation was scored in both pEGFP-3a-transfected and pEGFP-C1 empty vector-transfected cells. We found that almost 90% of the green-fluorescent pEGFP-3a-transfected cells showed chromatin alterations. We used the Pearson χ^2 test to analyse the differences in the numbers of GFP-positive cells with chromatin condensation. We found that the chromatin condensation was probably due to the apoptotic effect of the 3a protein, rather than to the presence of GFP, as the *P* value was less than 0.001 (Fig. 3c).

Induction of DNA fragmentation by the 3a protein

To examine whether the 3a protein induced DNA fragmentation, a common phenomenon of apoptosis, Vero E6 cells were transfected transiently with pcDNA4-3a. The expression level of the 3a protein and possible internucleosomal DNA cleavage were monitored daily for 5 days. Overexpression of the 3a protein was analysed by using the anti-3a antibody. Although 3a protein expression was detected from days 1–4 post-transfection, with peak expression observed on day 2, extensive low-molecular-mass apoptotic DNA fragments were only observed from

day 3 onwards (Fig. 4a). There was no sign of DNA fragmentation in Vero E6 cells transfected with pcDNA4 empty vector, pcDNA4-HRPL29 (human ribosomal protein L29) or the mock-transfected controls (Fig. 4a). DNA fragmentation induced by staurosporin (250 nM), a potent protein kinase C inhibitor that activates the disruption of actin filaments (Takahashi *et al.*, 1998), served as a positive control (Fig. 4a). The anti-3a antibody recognized a single protein band with a size of approximately 35 kDa from 1 to 4 days post-transfection (Fig. 4b). Transfection of the pcDNA4 empty vector served as a negative control, whilst the pcDNA4-HRPL29 construct was used to monitor transfection efficiency. For pcDNA4-HRPL29-transfected cells, a protein band of the expected size (24 kDa) was observed from 1 to 4 days post-transfection (Fig. 4b). β -Actin was used as an internal loading control (Fig. 4b).

To confirm the effect of the 3a protein on DNA

fragmentation, a TUNEL assay was performed in 3a-transfected Vero E6 cells (Fig. 5). Extensive DNA fragmentation could be found in 3a-transfected cells from 3 days post-transfection and in the DNase I-induced positive control. Under the same exposure conditions, there was no sign of DNA fragmentation in the mock-transfected and pcDNA4 empty vector-transfected controls.

Activation of pro-caspase-8 by the 3a protein

Apoptosis can be activated through either the mitochondrion-mediated (Gross *et al.*, 1999) or the receptor-mediated (Ashkenazi & Dixit, 1998) pathway. To delineate the pathway by which the 3a protein might be involved in the induction of apoptosis, we examined the expression levels of Bcl-2 family proteins and caspase-8, which are common mediators of the mitochondrion- and receptor-mediated pathways, respectively. We found that cleavage of pro-caspase-8 was increased in 3a-transfected

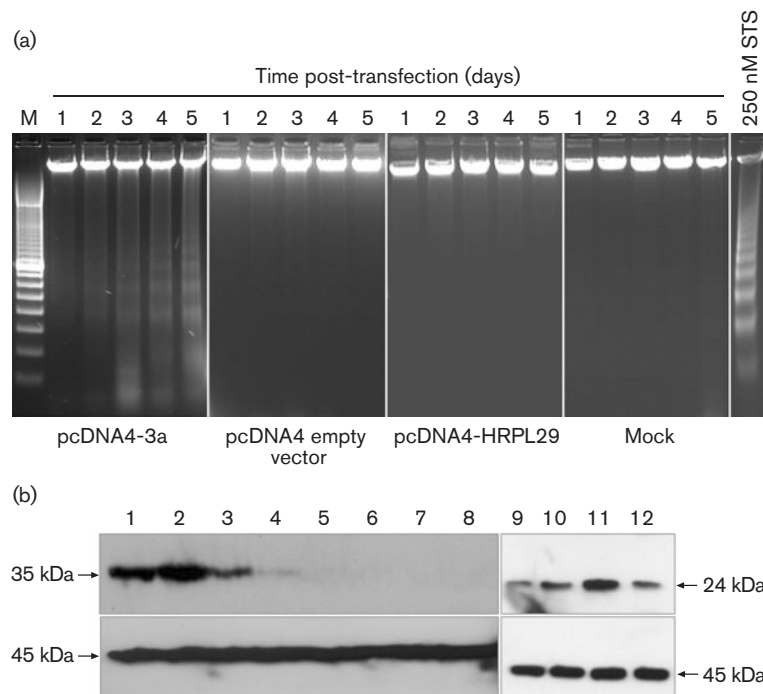


Fig. 4. DNA fragmentation in Vero E6 cells induced by the 3a protein. (a) The 3a protein induces apoptosis in mammalian cells. Lane M, 100 bp ladder molecular markers. Lanes 1–5, cells collected daily for 5 days post-transfection and analysed for DNA fragmentation. Apoptotic laddering was observed in pcDNA4-3a-transfected Vero E6 cells from 3 days post-transfection onwards. No low-molecular-mass DNA fragments were observed following transfection of pcDNA4 empty vector, pcDNA4-HRPL29 or the mock control. Induction of DNA fragmentation by treating Vero E6 cells in 250 nM staurosporin (STS) for 24 h served as a positive control. (b) Western blot analysis was performed to examine expression of the 3a protein. Approximately 25 μ g total cell lysate was loaded in each lane. The upper panel shows expression of the 3a protein (lanes 1–8) and HRPL29 (lanes 9–12). The lower panel shows detection of β -actin as loading control. Lanes 1–5, whole-cell lysates prepared from pcDNA4-3a-transfected Vero E6 cells from 1 to 5 days post-transfection; lanes 6–8, whole-cell lysates prepared from pcDNA4 empty vector-transfected Vero E6 cells from 1 to 3 days post-transfection (negative control); lanes 9–12, whole-cell lysates from pcDNA4-HRPL29-transfected Vero E6 cells from 1 to 4 days post-transfection. The 3a protein was recognized by the anti-3a antibody as a single protein band with a size of approximately 35 kDa, whilst HRPL29 was detected by using anti-His-G (Invitrogen Life Technologies) as a single protein band with a size of approximately 24 kDa.

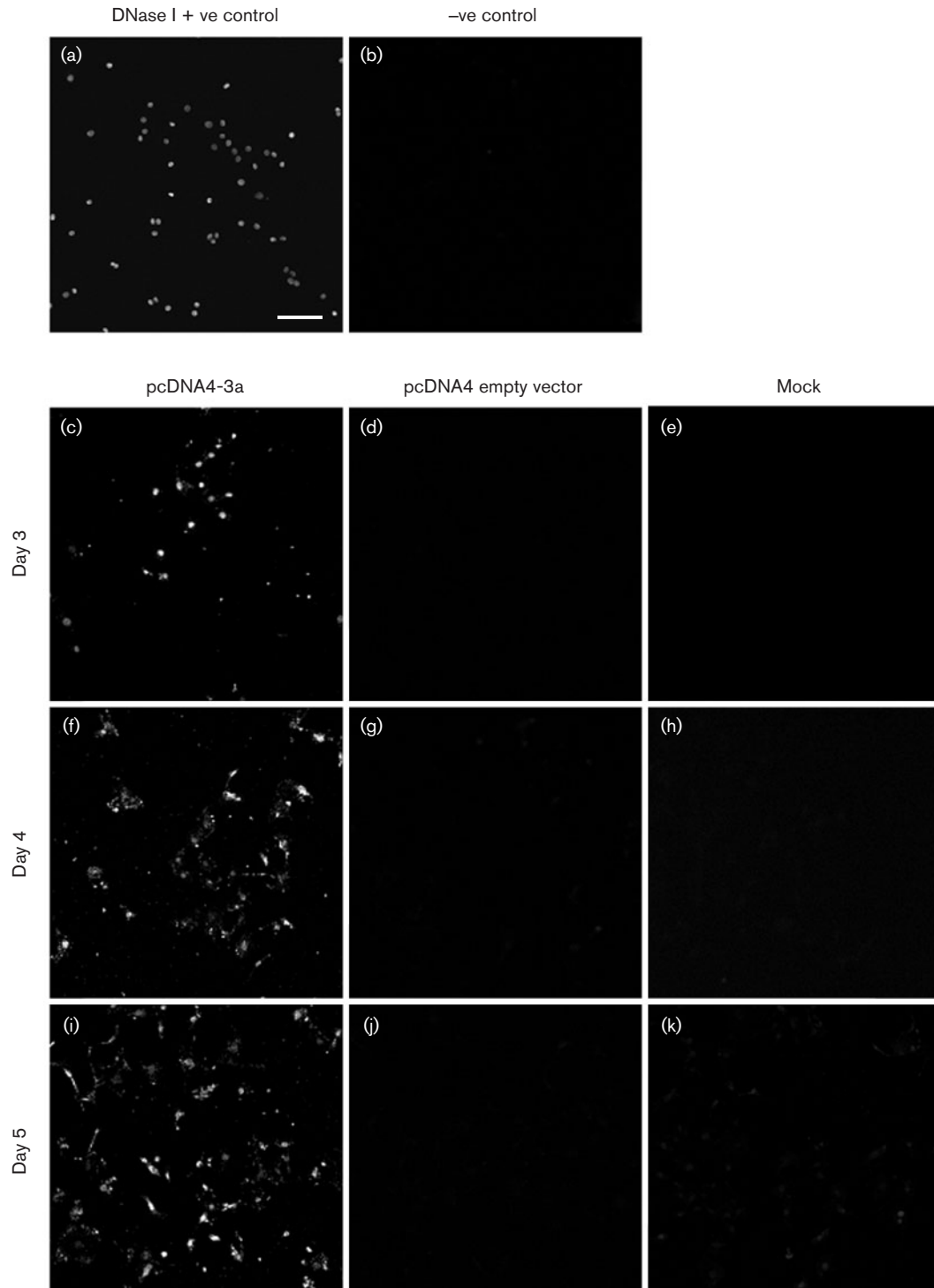


Fig. 5. TUNEL assay of pcDNA4-3a-transfected Vero E6 cells. (a, b) DNase I-treated positive control (a) and untreated negative control (b). (c–k) Transfection of pcDNA4-3a, pcDNA4 empty vector and mock transfection, respectively, at days 3 (c–e), 4 (f–h) and 5 (i–k) post-transfection. Bar, 50 μ m.

Vero E6 cells from 1 to 3 days post-transfection (Fig. 6). However, there were no effects on the endogenous levels of Bcl-2 family proteins such as Bcl-2 and Bad, and on

proliferating-cell nuclear antigen (PCNA) (a protein functioning in cell-cycle progression, DNA repair and replication) (Fig. 6).

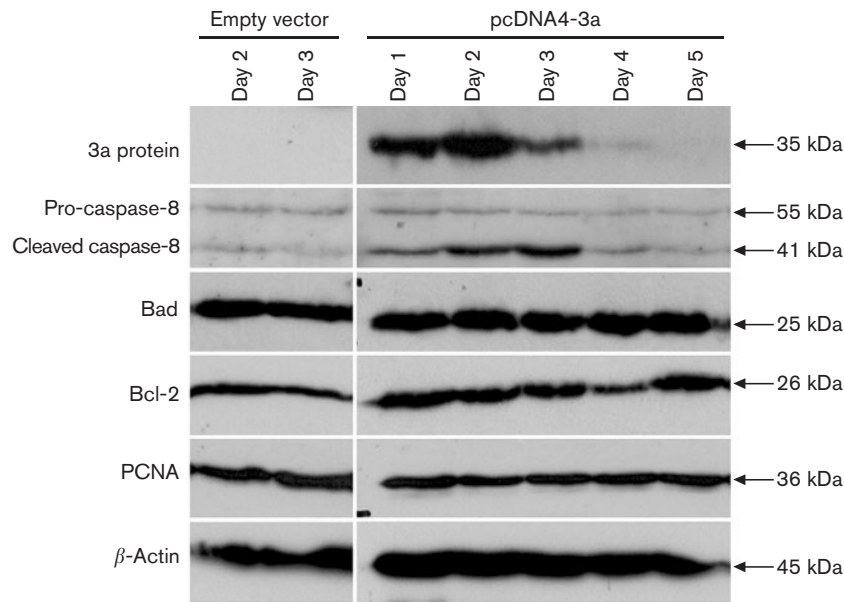


Fig. 6. Pro-caspase-8 activation in Vero E6 cells induced by the 3a protein. Western blot analysis was performed to analyse the cleavage of pro-caspase-8 in 3a-transfected Vero E6 cells. The expression levels of 3a protein from 1 to 5 days post-transfection were examined, and total cell lysate from empty pcDNA4-transfected Vero E6 cells (from 2 to 3 days post-transfection) was used as a negative control (left panel). Cleavage of pro-caspase-8 and endogenous levels of Bad, Bcl-2, PCNA and β -actin (loading control) from days 1 to 5 are shown.

DISCUSSION

In this study, we sought to analyse the apoptotic effect of the 3a protein, encoded by the largest ORF in the SARS-CoV genome. The 3a gene is located between two structural genes encoding the SARS-CoV spike and envelope proteins (Marra *et al.*, 2003). Consistent with a previous report (Yu *et al.*, 2004), our immunohistochemical data indicated the presence of the 3a protein in lung and intestinal specimens of SARS-CoV-infected patients.

Sequence analysis has suggested that the 3a protein contains an N-terminal signal sequence and three transmembrane domains. Although the 3a protein was reported to be localized in the perinuclear region and plasma membrane (Tan *et al.*, 2004a), others have suggested that the 3a protein is distributed in the cytoplasm and Golgi apparatus (Yu *et al.*, 2004). In contrast to these findings, our results indicated that the 3a protein localized to the ER. The discrepancy in subcellular localization may be due to differences in the specificities of antibodies being used. Another possible explanation is the involvement of the 3a protein in different subcellular compartments, as it probably is a multifunctional protein. Most notably, the 3a protein is unique to SARS-CoV and there is no homologue in other coronaviruses, which may explain the unexpectedly high virulence of SARS-CoV. The 3a protein has a cysteine-rich region located at the junction of the transmembrane and cytoplasmic regions, which can facilitate the formation of inter-chain disulfide bonds with the spike protein and may play an important role in the virulence of SARS-CoV (Zeng *et al.*, 2004). In addition, Tan *et al.* (2004a) suggested that the 3a protein can interact with structural proteins and may participate in virus assembly and propagation. Thus, the 3a protein may play different roles in virus virulence and assembly, as well as in the induction of apoptosis.

Apoptosis is an important host-defence mechanism that controls viral infection (O'Brien, 1998; Roulston *et al.*, 1999). However, virus-induced apoptosis can limit the inflammatory response and somehow facilitate the dissemination of progeny undetected by the host immune system (O'Brien, 1998). Many RNA viruses are known to induce apoptosis and this can play an important role in viral pathogenesis (Mori *et al.*, 2004). For instance, human immunodeficiency virus induces apoptotic cell death in T cells (Plymale *et al.*, 1999a, b) and influenza virus induces apoptosis in cultured MDCK and U937 cells (Price *et al.*, 1997), whilst Dengue virus causes apoptotic cell death in hepatoma cell lines (Marianneau *et al.*, 1997, 1998) and rubella virus provokes programmed cell death in Vero E6 cells (Hofmann *et al.*, 1999). Apoptotic cell death has been reported in SARS-CoV-infected Vero E6 cells (Yan *et al.*, 2004) and upregulation of apoptotic genes is observed in SARS-CoV-infected human peripheral blood mononuclear cells (Ng *et al.*, 2004). However, the precise mechanism and the viral protein(s) involved remain largely unknown. Recently, the nucleocapsid protein and the non-structural protein ORF7a have been shown to induce apoptosis when overexpressed in COS-1 and Vero E6 cells, respectively (Surjit *et al.*, 2004; Tan *et al.*, 2004b). Here, we have demonstrated for the first time that the non-structural protein 3a alone can induce apoptosis in SARS-CoV-susceptible Vero E6 cells.

Although expression of the 3a protein in mammalian cells was reported to be unsuccessful without the use of the vaccinia virus-infected transfection method (Yu *et al.*, 2004), we detected 3a protein expression in various cell lines, including Vero E6 cells, by using a simple transient transfection, and the recombinant 3a protein migrated as a single-band protein with a size of approximately 35 kDa. The time lag between peak expression of the 3a protein

(Fig. 4b) and the appearance of DNA fragmentation (Figs 4a and 5) is possibly due to the fact that DNA fragmentation is a late apoptotic event. Our study has shown that overexpression of the 3a protein can induce chromatin condensation and low-molecular-mass apoptotic DNA fragmentation from 3 days post-transfection. These data were consistent with the results of the TUNEL assay, showing a significant amount of internucleosomal DNA cleavage from 3 days post-transfection. As the receptor-mediated apoptotic pathway is Bcl-2-insensitive (Chen & Makino, 2002) and we found that caspase-8 (an apical caspase in the death-receptor apoptotic pathway) was activated, we postulate that overexpression of the 3a protein induces apoptosis, mediated through a caspase-8-dependent pathway, which may be similar to the death-receptor signalling cascades.

Analyses of the 3a protein has shown that it is homologous to the *Shewanella* outer-membrane porin and the *Plasmodium* calcium pump; therefore, we speculate that the 3a protein may alter membrane calcium-ion permeability. Calcium ions released from the ER perturb the ER/cytosolic calcium gradient and increase the cytosolic calcium concentration, which subsequently leads to ER stress-induced apoptosis (Breckenridge *et al.*, 2003). This may provide another possible mechanism of 3a-induced apoptosis.

In summary, the 3a protein was detected in lung and intestinal specimens of SARS patients. We demonstrated that the 3a protein is an ER membrane-bound protein that can induce apoptosis thorough a caspase-8-dependent pathway in Vero E6 cells. The present study provides a molecular link between SARS and apoptosis, and further investigations are needed to define in more detail the functional role of the 3a protein in SARS infection.

ACKNOWLEDGEMENTS

This project team is supported by the Research Fund for the Control of Infectious Diseases (RFCID) from the Health, Welfare and Food Bureau of the Hong Kong SAR Government.

REFERENCES

- An, S., Chen, C.-J., Yu, X., Leibowitz, J. L. & Makino, S. (1999). Induction of apoptosis in murine coronavirus-infected cultured cells and demonstration of E protein as an apoptosis inducer. *J Virol* **73**, 7853–7859.
- Ashkenazi, A. & Dixit, V. M. (1998). Death receptors: signaling and modulation. *Science* **281**, 1305–1308.
- Breckenridge, D. G., Germain, M., Mathai, J. P., Nguyen, M. & Shore, G. C. (2003). Regulation of apoptosis by endoplasmic reticulum pathways. *Oncogene* **22**, 8608–8618.
- Chau, T.-N., Lee, K.-C., Yao, H. & 8 other authors (2004). SARS-associated viral hepatitis caused by a novel coronavirus: report of three cases. *Hepatology* **39**, 302–310.
- Chen, C.-J. & Makino, S. (2002). Murine coronavirus-induced apoptosis in 17Cl-1 cells involves a mitochondria-mediated pathway and its downstream caspase-8 activation and bid cleavage. *Virology* **302**, 321–332.
- Eléouët, J.-F., Slee, E. A., Saurini, F., Castagné, N., Poncet, D., Garrido, C., Solary, E. & Martin, S. J. (2000). The viral nucleocapsid protein of transmissible gastroenteritis coronavirus (TGEV) is cleaved by caspase-6 and -7 during TGEV-induced apoptosis. *J Virol* **74**, 3975–3983.
- Gross, A., McDonnell, J. M. & Korsmeyer, S. J. (1999). BCL-2 family members and the mitochondria in apoptosis. *Genes Dev* **13**, 1899–1911.
- Hofmann, J., Pletz, M. W. R. & Liebert, U. G. (1999). Rubella virus-induced cytopathic effect *in vitro* is caused by apoptosis. *J Gen Virol* **80**, 1657–1664.
- Letunic, I., Copley, R. R., Schmidt, S., Ciccarelli, F. D., Doerks, T., Schultz, J., Ponting, C. P. & Bork, P. (2004). SMART 4.0: towards genomic data integration. *Nucleic Acids Res* **32**, D142–D144.
- Liu, C., Xu, H. Y. & Liu, D. X. (2001). Induction of caspase-dependent apoptosis in cultured cells by the avian coronavirus infectious bronchitis virus. *J Virol* **75**, 6402–6409.
- Liu, Y., Cai, Y. & Zhang, X. (2003). Induction of caspase-dependent apoptosis in cultured rat oligodendrocytes by murine coronavirus is mediated during cell entry and does not require virus replication. *J Virol* **77**, 11952–11963.
- Marianneau, P., Cardona, A., Edelman, L., Deubel, V. & Després, P. (1997). Dengue virus replication in human hepatoma cells activates NF- κ B which in turn induces apoptotic cell death. *J Virol* **71**, 3244–3249.
- Marianneau, P., Flamand, M., Deubel, V. & Després, P. (1998). Induction of programmed cell death (apoptosis) by dengue virus *in vitro* and *in vivo*. *Acta Cient Venez* **49** (Suppl. 1), 13–17.
- Marra, M. A., Jones, S. J. M., Astell, C. R. & 56 other authors (2003). The genome sequence of the SARS-associated coronavirus. *Science* **300**, 1399–1404.
- Mori, I., Nishiyama, Y., Yokochi, T. & Kimura, Y. (2004). Virus-induced neuronal apoptosis as pathological and protective responses of the host. *Rev Med Virol* **14**, 209–216.
- Ng, L. F. P., Hibberd, M. L., Ooi, E.-E. & 8 other authors (2004). A human *in vitro* model system for investigating genome-wide host responses to SARS coronavirus infection. *BMC Infect Dis* **4**, 34.
- O'Brien, V. (1998). Viruses and apoptosis. *J Gen Virol* **79**, 1833–1845.
- O'Donnell, R., Tasker, R. C. & Roe, M. F. E. (2003). SARS: understanding the coronavirus. Apoptosis may explain lymphopenia of SARS. *BMJ* **327**, 620.
- Panesar, N. S., Lam, C. W. K., Chan, M. H. M., Wong, C. K. & Sung, J. J. Y. (2004). Lymphopenia and neutrophilia in SARS are related to the prevailing serum cortisol. *Eur J Clin Invest* **34**, 382–384.
- Plymale, D. R., Comardelle, A. M., Fermin, C. D. & 7 other authors (1999a). Concentration-dependent differential induction of necrosis or apoptosis by HIV-1 lytic peptide 1. *Peptides* **20**, 1275–1283.
- Plymale, D. R., Ng Tang, D. S., Comardelle, A. M., Fermin, C. D., Lewis, D. E. & Garry, R. F. (1999b). Both necrosis and apoptosis contribute to HIV-1-induced killing of CD4 cells. *AIDS* **13**, 1827–1839.
- Price, G. E., Smith, H. & Sweet, C. (1997). Differential induction of cytotoxicity and apoptosis by influenza virus strains of differing virulence. *J Gen Virol* **78**, 2821–2829.
- Rota, P. A., Oberste, M. S., Monroe, S. S. & 32 other authors (2003). Characterization of a novel coronavirus associated with severe acute respiratory syndrome. *Science* **300**, 1394–1399.
- Roulston, A., Marcellus, R. C. & Branton, P. E. (1999). Viruses and apoptosis. *Annu Rev Microbiol* **53**, 577–628.

- Ruan, Y. J., Wei, C. L., Ee, L. A. & 17 other authors (2003). Comparative full-length genome sequence analysis of 14 SARS coronavirus isolates and common mutations associated with putative origins of infection. *Lancet* **361**, 1779–1785.
- Surjit, M., Liu, B., Jameel, S., Chow, V. T. K. & Lal, S. K. (2004). The SARS coronavirus nucleocapsid protein induces actin reorganization and apoptosis in COS-1 cells in the absence of growth factors. *Biochem J* **383**, 13–18.
- Takahashi, M., Mukai, H., Toshimori, M., Miyamoto, M. & Ono, Y. (1998). Proteolytic activation of PKN by caspase-3 or related protease during apoptosis. *Proc Natl Acad Sci U S A* **95**, 11566–11571.
- Tan, Y.-J., Teng, E., Shen, S. & 7 other authors (2004a). A novel severe acute respiratory syndrome coronavirus protein, U274, is transported to the cell surface and undergoes endocytosis. *J Virol* **78**, 6723–6734.
- Tan, Y.-J., Fielding, B. C., Goh, P.-Y., Shen, S., Tan, T. H. P., Lim, S. G. & Hong, W. (2004b). Overexpression of 7a, a protein specifically encoded by the severe acute respiratory syndrome coronavirus, induces apoptosis via a caspase-dependent pathway. *J Virol* **78**, 14043–14047.
- To, K. F., Tong, J. H. M., Chan, P. K. S. & 9 other authors (2004). Tissue and cellular tropism of the coronavirus associated with severe acute respiratory syndrome: an *in-situ* hybridization study of fatal cases. *J Pathol* **202**, 157–163.
- Tsui, S. K. W., Chim, S. S. C., Lo, Y. M. D. & Chinese University of Hong Kong Molecular SARS Research Group (2003). Coronavirus genomic-sequence variations and the epidemiology of the severe acute respiratory syndrome. *N Engl J Med* **349**, 187–188.
- Yan, H., Xiao, G., Zhang, J., Hu, Y., Yuan, F., Cole, D. K., Zheng, C. & Gao, G. F. (2004). SARS coronavirus induces apoptosis in Vero E6 cells. *J Med Virol* **73**, 323–331.
- Yeh, S.-H., Wang, H.-Y., Tsai, C.-Y. & 7 other authors (2004). Characterization of severe acute respiratory syndrome coronavirus genomes in Taiwan: molecular epidemiology and genome evolution. *Proc Natl Acad Sci U S A* **101**, 2542–2547.
- Yu, C.-J., Chen, Y.-C., Hsiao, C.-H. & 9 other authors (2004). Identification of a novel protein 3a from severe acute respiratory syndrome coronavirus. *FEBS Lett* **565**, 111–116.
- Zeng, F. Y., Chan, C. W. M., Chan, M. N. & 15 other authors (2003). The complete genome sequence of severe acute respiratory syndrome coronavirus strain HKU-39849 (HK-39). *Exp Biol Med (Maywood)* **228**, 866–873.
- Zeng, R., Yang, R.-F., Shi, M.-D. & 31 other authors (2004). Characterization of the 3a protein of SARS-associated coronavirus in infected Vero E6 cells and SARS patients. *J Mol Biol* **341**, 271–279.